Fundamental-Mode Pierce Oscillators Utilizing Bulk-Acoustic-Wave Resonators in the 250–300-MHz Range

STANLEY G. BURNS AND RICHARD S. KETCHAM

Abstract—**Fundamental-mode Pierce oscillators in the 250–300-MHz range have been realized utilizing a unique form of a bulk-acoustic-wave (BAW) resonator. Phase noise greater than −100 dBc/Hz (1-kHz offset) has been extrapolated from data collected on oscillators operating at −22 and −24 dBm. Higher power levels to +6 dBm have been achieved. A linear-model design was used. The circuit topology used and resonator fabrication technique shows great promise for the creation of MMIC circuits in the 200-MHz–2-GHz range.**

I. Introduction

THE FREQUENCY OF operation of fundamental-mode crystal-controlled oscillators is restricted to the relatively low resonant frequencies of the crystal. Typically, those fundamental modes are several 10's of MHz, though ion-beam milling techniques have been used to fabricate quartz resonators operating to 500 MHz [1]. This paper describes the design and operation of a Pierce oscillator using a unique form of a bulk-acoustic-wave (BAW) resonator composed of a thin film of ZnO sputtered onto a thin Si-membrane supporting structure [2]. This device, illustrated in Fig. 1, has been fabricated with fundamental resonances from 200 MHz to over 1 GHz with Q's greater than 9000. Preliminary results have been achieved using discrete circuit techniques on 250–300-MHz oscillators. These results and design procedures are described in this paper.

II. Oscillator Design

The diagram of a Pierce oscillator is shown in Fig. 2. We show an active device that is used to sustain oscillations when constrained by the feedback network composed of the input tuning capacitor C_i, the output tuning capacitor C_o, and the BAW resonator. The operating frequency is just above the series-resonant frequency of the resonator where good frequency stability is achieved due to the resonator's high-Q and resultant steep phase characteristic.

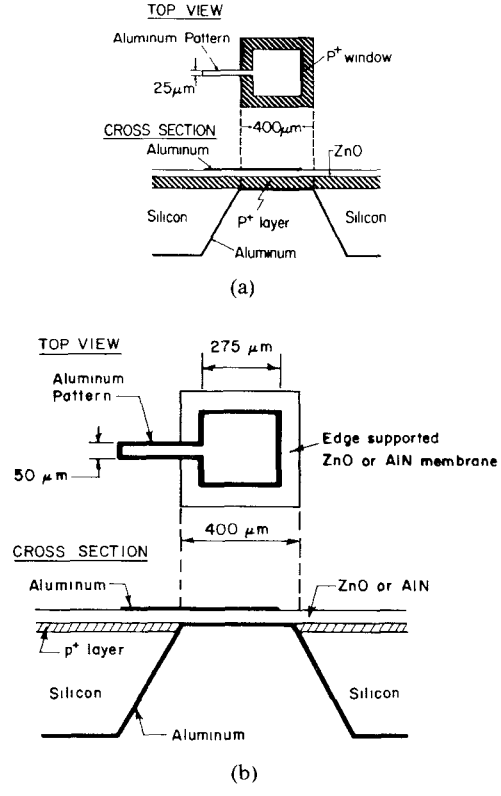

Fig. 1. Schematic of thin-film composite resonator.

Analyses of this circuit are usually performed for low frequencies utilizing simplifications that allow compact design equations [3]. Chief among these simplifications are that the active device is considered to be unilateral and that the resonator is lossless. When various conditions of the circuit are altered, such as the operating frequency or the type of active device (bipolar versus GaAs FET), many of the original simplifications don't apply and the design equations are of limited use. Oscillators designed for maximum power, preferable when optimizing a given oscillator configuration, require large-signal measurements or extensive numerical modeling [4]–[6]. The design approach utilizes a general, linear, small-signal y-parameter model to predict the onset of oscillation by satisfying the Barkhausen criteria.

Manuscript received April 30, 1984; revised July 25, 1984. This work was supported in part by the Air Force Office of Scientific Research and the Iowa State University Engineering Research Institute.

S. G. Burns is with the Department of Electrical and Computer Engineering, Iowa State University, Ames, Iowa 50011.

R. S. Ketcham is with the Mass Storage Peripherals Group, Hewlett Packard Corporation, Greeley, CO 80631.

0018-9480/84/1200-1668$01.00 ©1984 IEEE

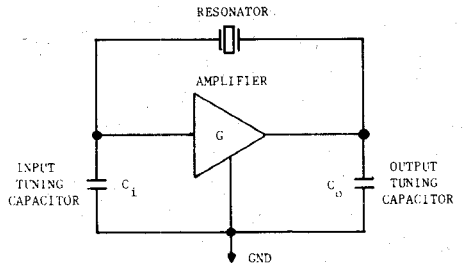

Fig. 2. Generalized Pierce oscillator.

The y-parameter model, illustrated in Fig. 3, shows two interconnected networks: the reactance tuning network (network B), and the composite active device network (network A). The active device and feedback resonator are considered as a composite device because their individual y-parameters are directly measurable. Given the y-parameters of network A, susceptances of network B can be directly solved that satisfy the Barkhausen criteria.

Let the composite active device, network A in Fig. 3, be represented by its y-parameter matrix

$$y_A = \begin{bmatrix} (g_{iA} + jb_{iA}) & (g_{rA} + jb_{rA}) \\ (g_{fA} + jb_{fA}) & (g_{oA} + jb_{oA}) \end{bmatrix}. \tag{1}$$

Also, consider the input and output tuning capacitors, illustrated by network B in Fig. 3, as tuning susceptances, and represent them by

$$y_B = \begin{bmatrix} jb_{iB} & 0 \\ 0 & jb_{oB} \end{bmatrix}. \tag{2}$$

Because of the shunt-shunt interconnection of the two networks used in the model, we arrive at the oscillation condition by adding the elements of the two matrices and applying the Barkhausen criteria

$$y_{11}y_{22} - y_{12}y_{21} = 0 \tag{3}$$

or

$$[g_{iA} + j(b_{iA} + b_{iB})][g_{oA} + j(b_{oA} + b_{oB})] - (g_{rA} + jb_{rA})(g_{fA} + jb_{fA}) = 0. \tag{4}$$

When (4) is expanded and real and imaginary terms are collected, the results are

$$(b_{iB} + b_{iA})(b_{oB} + b_{oA}) = g_{iA}g_{oA} + b_{rA}b_{fA} - g_{fA}g_{rA} \tag{5a}$$

$$b_{iB}g_{oA} + b_{oB}g_{iA} = g_{rA}b_{fA} + b_{rA}g_{fA} - g_{iA}b_{oA} - b_{iA}g_{oA}. \tag{5b}$$

When the y-parameters of the composite active device, network A, are known, (5a) represents a hyperbola and (5b) represents a straight line in terms of the tuning susceptances b_{iB} and b_{oB}. Equations (5a) and (5b) are solved simultaneously for either b_{iB} or b_{oB} by substitution. Solving for b_{oB}

$$b_{oB}^2(g_{iA}) + b_{oB}(g_{iA}b_{oA} - b_{iA}g_{oA} - K_2) + (K_1 - K_2b_{oA} - b_{iA}g_{oA}b_{oA}) = 0. \tag{6}$$

This represents a second-order polynomial in b_{oB} and is

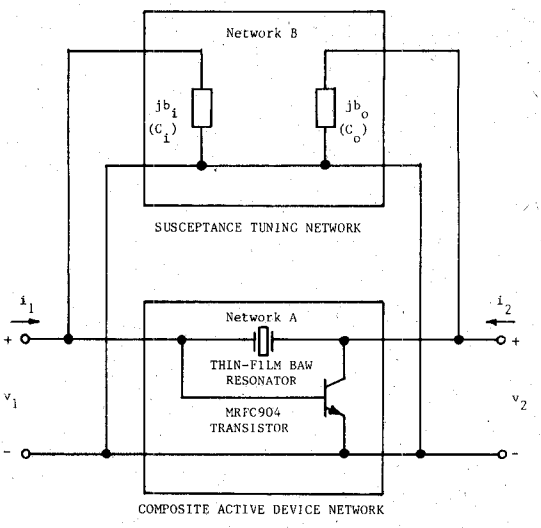

Fig. 3. Y-parameter model for Pierce oscillator.

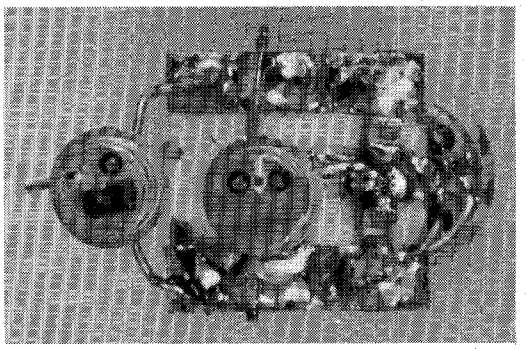

Fig. 4. Photograph of 259-MHz Pierce oscillator.

solved using the quadratic equation

$$b_{oB} = \left(-b \pm [b^2 - 4ac]^{1/2}\right)/2a \tag{7}$$

where

$$K_1 = g_{iA}g_{oA} + b_{rA}b_{fA} - g_{rA}g_{fA} \tag{8a}$$

$$K_2 = g_{rA}b_{fA} + b_{rA}g_{fA} - g_{iA}b_{oA} - b_{iA}g_{oA} \tag{8b}$$

$$a = g_{iA} \tag{8c}$$

$$b = g_{iA}b_{oA} - b_{iA}g_{oA} - K_2 \tag{8d}$$

$$c = K_1 - K_2b_{oA} - b_{iA}g_{oA}b_{oA}. \tag{8e}$$

Only solutions where b_{iB} and b_{oB} represent capacitive susceptances are utilized.

Because this analysis is based on linear small-signal y-parameters, not all solutions arrived at will result in stable oscillations. Some of the solutions, which predict initial instability, do not result in stable limit-cycles. A rigorous solution would have to incorporate a nonlinear model.

III. Experimental Results

A series of Pierce oscillators were built, using discrete elements, according to (5a) and (5b). An example is shown in Fig. 4. This circuit consists of a TO-18-mounted composite BAW resonator (top header), a TO-18-mounted

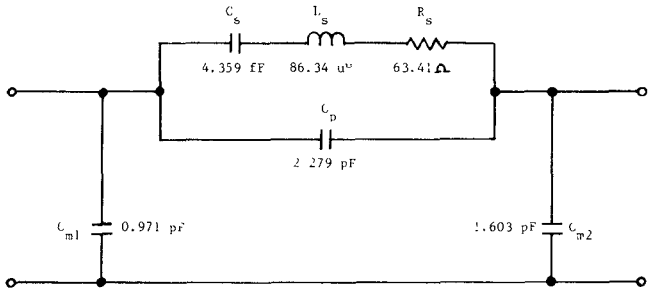

Fig. 5. Model of 259-MHz TO-18 resonator.

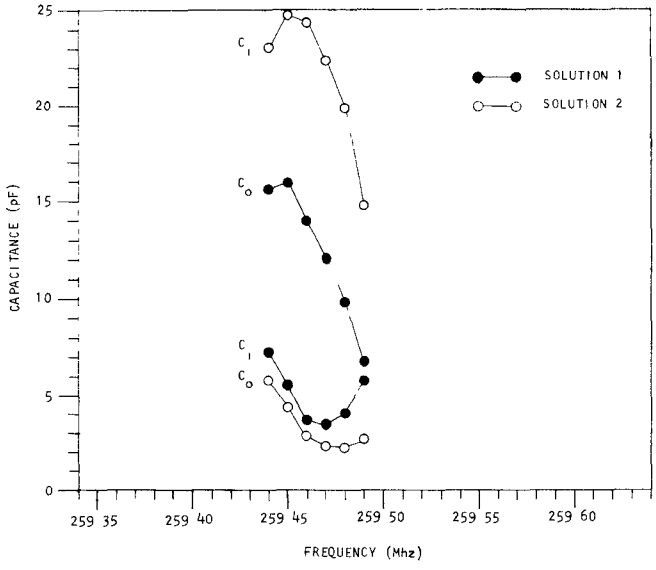

Fig. 6. Computed solution curves for C_o and C_t.

MRFC904 chip transistor (bottom header), and the input and output RF chip capacitors. Oscillator bias and output matching components, not shown in Fig. 4, are contained within the bias-test stand. The components are mounted on an 11.4-mm-square alumina substrate epoxied to a TO-5 header with circuit interconnections realized with copper foil. Discrete components were used in the oscillator so that y-parameter data could be collected on the individual devices.

Data from candidate composite resonators and active devices were obtained using an HP8505 network analyzer. Data are collected from resonators mounted on the substrate to ensure that stray parasitics are considered during the design process. An equivalent model for a substrate-mounted composite resonator is shown in Fig. 5. This resonator has a series resonant frequency of 259.39 MHz, a parallel resonant frequency of 259.63 MHz, and a computed Q of 2200. In this figure, C_{m1} and C_{m2} represent the mounting parasitics. These parasitics typically are not equal due to asymmetries in the resonator mounting. The transistor is tested as a discrete device at a frequency close to the series resonance of the resonator.

The required values for C_o and C_t are computed as a function of frequency using (5) and (6). A sample solution set for the required capacitors is shown in Fig. 6 for the resonator modeled in Fig. 5.

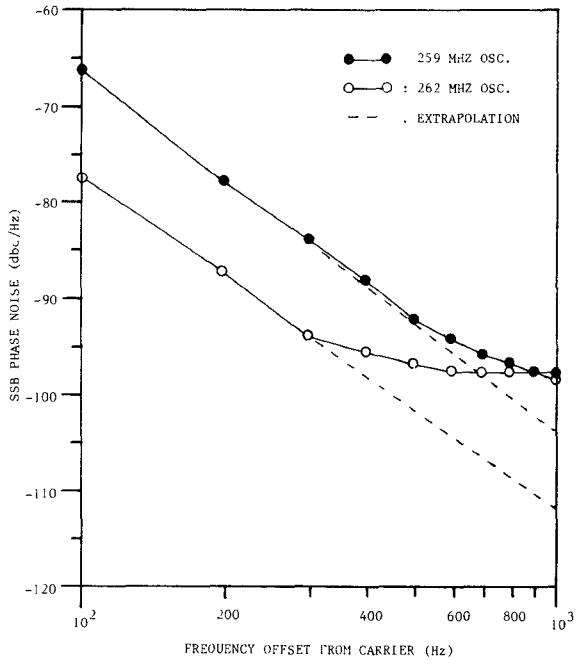

Fig. 7. Measured phase-noise characteristics of Pierce oscillators.

Fig. 7 shows the SSB phase-noise characteristics, measured with an HP8566A spectrum analyzer of two oscillators using MRFC904 chip transistors. For the 259-MHz oscillator, the computed Q of the resonator is 2200 and the value of C_o is 3 pF. The output power level is -24 dBm. At a frequency offset of 100 Hz, the measured phase noise is -66 dBc/Hz. For the 262-MHz oscillator, the computed Q of the resonator is 2400 and the value of C_o is 15 pF. The output power level is -22 dBm. The values required for C_o and C_t were in good agreement with the computed solution (Fig. 6). Q is computed from measured equivalent circuit elements (Fig. 5). At a frequency offset of 100 Hz, the measured phase noise is -77 dBc/Hz. Both phase-noise curves tend to flatten out at higher offset frequencies due to the dynamic range limitations of the HP8566A and the test fixture; hence, the need to extrapolate these data. While testing the oscillators, it was observed that their spectra and the spectrum of a synthesizer approached the same noise floor. Based upon a linear extrapolation of the near-in data (100–300-Hz offsets), the computed phase noise at a 1-kHz offset is 104 dBc/Hz for the 259-MHz oscillator and a -112 dBc/Hz for the 2652-MHz oscillator. When allowed to self-stabilize within a thermal chamber, frequency stabilities of 1.9×10^{-8} were observed based on a 4-min sample period.

These data should be considered "worst case" because the circuits contain no thermal bias stabilization and the noise measurements did not rigorously correct for test equipment induced noise.

IV. Conclusion and Future Work

This paper has described a fundamental-mode UHF oscillator utilizing a thin-film BAW resonator. This is the first application of the thin-film BAW technology. Additional work is currently underway in the areas of nonlin-

ear modeling, noise modeling, and temperature stabilization of hybrid and monolithic UHF oscillators utilizing composite resonators. Wang *et al.* [7] have recently described a similar resonator structure with temperature stabilities exceeding AT-cut quartz. Since composite bulk wave resonators have been demonstrated at frequencies above 1 GHz [8], work is now proceeding on fundamental-mode hybrid circuits at these frequencies. It is expected that integrated-circuit fabrication techniques will permit direct integration of the resonator with active devices on the same substrate resulting in a new class of RF/LSI-type circuits. Work is proceeding in this area.

ACKNOWLEDGMENT

The authors wish to thank Dr. K. Lakin and A. Landin of Ames Laboratory for their technical assistance in building the oscillator, and the Metrology Standards Laboratory of Rockwell International for the noise measurements.

REFERENCES

[1] M. Berte, *Electron. Lett.*, vol. 13, p. 248, 1977.
[2] K. M. Lakin and J. S. Wang, "Acoustic bulk wave composite resonators," *Appl. Phys. Lett.*, vol. 38(3), Feb. 1, 1981.
[3] M. E. Frerking, *Crystal Oscillator Design and Temperature Compensation*. New York: Van Nostrand Reinhold, 1978, App. B.
[4] D. F. Page and A. R. Boothroyd, "Instability in two-port active networks," *IRE Trans. Circuit Theory*, pp. 133–139, June 1958.
[5] M. Vehovec, L. Houselander, and R. Spence, "On oscillator design for maximum power," *IRE Trans. Circuit Theory*, pp. 281–283, Sept. 1968.
[6] R. J. Gilmore and F. J. Rosenbaum, "An analytic approach to optimum oscillator design using *S*-parameters," *IEEE Trans. Microwave Theory Tech.*, pp. 633–639, Aug. 1983.
[7] J. S. Wang, A. R. Landin, and K. M. Lakin, "Low temperature coefficient shear wave thin films for composite resonators and filters," in *IEEE 1983 Ultrasonics Symposium Proc.*
[8] G. R. Kline and K. M. Lakin, "1.0 GHz thin film bulk acoustic wave resonators on GaAs," *Appl. Phys. Lett.*, vol. 43(8), Oct. 15, 1983.

YIG Oscillators: Is a Planar Geometry Better?

RONALD L. CARTER, MEMBER, IEEE, JOHN M. OWENS, MEMBER, IEEE, AND D. K. DE

Abstract—**Two yttrium–iron–garnet (YIG) oscillator technologies are compared: the more mature YIG sphere oscillator technology which is based on the uniform (resonant) precession of the electron spins in a small sphere of YIG, and the new planar YIG technology which utilizes the propagation of magnetostatic waves in an epitaxial film of YIG. The YIG sphere technology has been used for microwave oscillators for more than 25 years, but has two significant areas of difficulty in applications: the alignment of the YIG sphere in the magnetic bias field coupling cavity requires great precision and the gain element requires a negative resistance element to sustain oscillation. The MSW technology is much newer and less well understood, but the resonator elements are fabricated using a 50-μm line width planar technology making it an appealing candidate. Both technologies are reviewed herein with regard to resonant element theory, temperature, and noise characteristics. New data and theory are presented on MSW resonator optimization.**

I. BACKGROUND

OSCILLATORS using YIG spheres (YTO) have been made for more than 25 years. Recently, Zensius [1] reported a design for a YTO operating up to 40 GHz. The YTO sphere technology is quite mature. The YIG spheres are small (~ 0.5 mm diam), so the associated magnet designs are not overly complex. Considerable work has been reported on the choice of an orientation axis of the magnetic field for optimum temperature compensation. There are two design considerations that are not easy to overcome, however. The common choice for the resonator configuration is a one-port design, so the gain element must be operated in a negative resistance mode, as shown in Fig. 1. Also, the magnetic-field orientation and coupling loop alignments are rather complex, three-dimensional alignment procedures. The small size of the sphere and coupling loop means that the precision is comparable to watchmaking.

The advent of magnetostatic wave devices [2], [3] has included resonator elements fabricated in this planar technology. One apparent advantage of the planar versus the sphere resonators is that the loaded Q's are a factor of 5 larger for the planar resonators than for the sphere (~ 1000 versus 200). The magnetic field required at a given frequency for resonance is somewhat lower for the planar resonators. The planar resonators are more easily fabricated than the sphere resonators, the processing being exactly analogous to the MIC fabrication procedures. MSW

Manuscript received May 31, 1984. This work was supported in part by the Air Force Office of Scientific Research (RADC) and by Wavetek.

The authors are with the Electrical Engineering Department, University of Texas at Arlington, Arlington, TX 76019.

0018-9480/84/1200-1671$01.00 ©1984 IEEE